

Orbital Angular Momentum Parton Distributions in Light-Front Dynamics

F. Cano¹, P. Faccioli^{2,3}, S. Scopetta² and M. Traini^{1,4}

¹Dipartimento di Fisica
Università degli Studi di Trento
I-38050 Povo, Italy.

² ECT*,
European Centre for Theoretical Studies
in Nuclear Physics and Related Areas,
Villa Tambosi, I-38050 Villazzano (Trento), Italy.

³ Department of Physics and Astronomy,
State University of New York at Stony Brook, USA.

⁴ Istituto Nazionale di Fisica Nucleare, G.C. Trento.

Abstract

We study the quark angular momentum distribution in the nucleon within a light-front covariant quark model. Special emphasis is put into the orbital angular momentum: a quantity which is very sensitive to the relativistic treatment of the spin in a light-front dynamical approach. Discrepancies with the predictions of the low-energy traditional quark models where relativistic spin effects are neglected, are visible also after perturbative evolution to higher momentum scales. Orbital angular momentum distributions and their contribution to the spin sum rule are calculated for different phenomenological mass operators and compared with the results of the MIT bag model.

PACS: 12.39.-x, 12.39.Ki, 13.88.+e

Keywords: Orbital angular momentum, light-front quark models, parton distributions.

Preprint UTF-438,ECT*-00-002

1 Introduction

The EMC measurement of the integrated helicity parton distributions [1] (for recent results at SLAC see [2]) triggered the interest in a deeper understanding of how the total angular momentum of the nucleon is shared among its constituents. It was found that the fraction of the nucleon spin carried by the quarks was rather small, at variance with the most naive quark model expectation where the proton spin is (almost) entirely built from the spin of the quarks. Among the different explanations of these discrepancies, it was proposed [3] that the (overlooked until then) polarization of the gluons might also contribute to the singlet axial charge through the axial anomaly. In that case, experimental data would be compatible with a rather large fraction of the spin carried by the quarks ($\Delta\Sigma = 0.45 \pm 0.09$ in a recent world data analysis [4]), though still far away from the non-relativistic quark model predictions.

One of the most important issues raised by the 'spin crisis' was the need for considering all the possible sources of angular momentum in the nucleon. Therefore, the spin sum rule should read [5, 6]:

$$\frac{1}{2}\Delta\Sigma(Q^2) + \Delta g(Q^2) + L_q(Q^2) + L_g(Q^2) = \frac{1}{2}, \quad (1)$$

where $\frac{1}{2}\Delta\Sigma(Q^2)$ ($\Delta g(Q^2)$) is the spin carried by the quarks and antiquarks (gluons) and $L_q(Q^2)$ ($L_g(Q^2)$) is the orbital angular momentum (OAM) contribution of the quarks (gluons) [7].

The significant role of OAM was pointed out several years ago [5, 8], but the problem was rigorously formulated only recently, when a gauge invariant definition of the quark and gluon (twist-two) operators was proposed [9, 10]. Besides, there has been a big effort to derive evolution equations (at one-loop level) for OAM observables [9, 11]. At the present there is only one gauge invariant definition of quark OAM [9] with known Q^2 evolution and experimentally accessible (for a discussion cfr. Ref. [12]). Such a definition holds for reference frames with definite nucleon polarization and the OAM distribution could be measured through the forward limit of skewed parton distributions.

One peculiar feature, already expected by general arguments [5, 8], is explicitly realized in the evolution equations, namely that the OAM distribution is coupled to the helicity parton distributions. As a consequence, OAM contributions can be generated, through evolution at higher scales, even in the case of vanishing OAM components at low initial hadronic scale. This is indeed the case for most hadronic models where the quarks are arranged, in the ground state, in a $l = 0$ S-wave configuration, stressing the crucial role of Q^2 evolution for the evaluation of spin observables or, in other words, the roughness of the identification of constituent quarks with partons at all energy scales.

From a quantitative point of view, some studies are currently available [13, 14, 15]. In particular, in ref. [13], the OAM distributions have been calculated for a number of hadronic models. As a first step these quantities are evaluated at the hadronic (low energy) scale and then evolved to the experimental $Q^2 \gg \mu_0^2$ scale by using the Leading Order (LO) evolution procedure recently established [9]. One central conclusion of that work is that a sizeable initial OAM distributions can deeply influence the final high-energy results. As a consequence, a clear difference arises between non-relativistic and relativistic models: while the former usually give a tiny OAM contribution at μ_0^2 , the latter may give rise to sizeable effects at high x that persist after evolution. To this respect, OAM distributions are useful quantities to assess the relevance of relativistic effects in the hadronic models of the nucleon.

In a recent study we investigated the consequences of a light-front treatment of relativistic spin effects on the helicity distributions [16, 17] and in the present paper we want to enlarge our analysis to OAM investigating in detail the predictions of a light-front covariant quark model. As a matter of fact, the spin dynamics can be discussed within the light-front approach in a way which respects covariance requirements and particularly suitable to discuss deep inelastic polarized processes, both at the hadronic [15, 16, 17] and high-energy (partonic) scale [16, 17]. We will show that light-front covariant quark models (LFCQM) predict a non-vanishing OAM distribution whose main features survive after evolution. We will also see that these predictions hold for a variety of mass operators indicating that the relevant ingredient is the relativistic treatment of the spin wave functions, absent in many traditional formulations of the quark model. The comparison with other relativistic models (MIT bag model) and the analysis of the moments that enter the spin sum rule will allow us to assess the reliability of LFCQM.

2 OAM at the hadronic scale

In the recent years a quark model-based approach has been developed for computing the non-perturbative inputs in the evolution equations [18] and describing polarized and unpolarized parton distributions. Schematically, the central assumption is that at some low-energy scale (μ_0^2) the nucleon is made up of valence quarks that can be identified with the constituents of the quark model (or the bag model in alternative treatments). Therefore, the non-perturbative boundary conditions can be evaluated by using low-energy models of the nucleon. Subsequent refinements led to the inclusion of non-perturbative gluons and sea at the hadronic scale μ_0^2 [19], as well as the explicit partonic content of the constituent quarks [20].

By following such a procedure we will assume that at the hadronic scale only valence quarks are resolved so that the quark helicity distribution $g_1^a(x, \mu_0^2)$

for a given flavour a is given in terms of the momentum density of the valence quarks:

$$g_1^a(x, \mu_0^2) = \frac{1}{(1-x)^2} \int d\vec{k} (n_a^\uparrow(\vec{k}) - n_a^\downarrow(\vec{k})) \delta\left(\frac{x}{1-x} - \frac{k^+}{M_N}\right), \quad (2)$$

where x is the Bjorken variable, M_N the mass of the nucleon and k^+ is defined as a function of the parton momentum as $k^+ = \sqrt{\vec{k}^2 + m^2} + k_z$. The polarized momentum densities are defined as:

$$n_a^{\uparrow\downarrow}(\vec{k}) = \langle N, J_z = 1/2 | \sum_{i=1}^3 \mathcal{P}_a \frac{1 \pm \sigma_z^{(i)}}{2} \delta(\vec{k}_i - \vec{k}) | N, J_z = 1/2 \rangle, \quad (3)$$

where \mathcal{P}_a is the flavour projector.

An analogous definition can be worked out for the OAM distributions [13]:

$$L_z(x, \mu_0^2) = \frac{1}{(1-x)^2} \int d\vec{k} L_z(\vec{k}) \delta\left(\frac{x}{1-x} - \frac{k^+}{M_N}\right), \quad (4)$$

where the density of the angular momentum is defined in the usual way:

$$L_z(\vec{k}) = \langle N, J_z = 1/2 | \sum_{i=1}^3 -i(\vec{k}_i \times \vec{\nabla}_{\vec{k}_i})_z \delta(\vec{k}_i - \vec{k}) | N, J_z = 1/2 \rangle. \quad (5)$$

From the previous definitions one can recover the result $L_z(x, \mu_0^2) = 0$ obtained assuming S-wave quarks only, and non-relativistic approximation (i.e. $L_z(\vec{k}) = 0$). A more complicated example within non-relativistic dynamics, is given by models whose nucleon wave function is a superposition of various $SU(6)$ components, such as the Isgur-Karl model [21]. The non-vanishing contribution to $L_z(\vec{k})$ in these cases is due to the D-state (or higher waves) admixture. For example, in the Isgur-Karl model, the OAM distribution of Eq. (4) results to be proportional to the D-State probability a_D^2 [13] and its contribution is very small ($a_D = -0.067$).

This situation is radically changed in a light-front covariant quark model. In light-front dynamics (LFD) [22], the specific partition of the Poincaré algebra into kinetic and Hamiltonian generators leads to several simplifications of the relativistic many-body problem such as, for example, the clean separation of the center of mass motion. The prize to pay is that the description of angular momentum is rather complicated. Not all the generators of rotations, in fact, belong to the kinetic subgroup, and hence the angular momentum operator is, in general, interaction dependent.

For this reason, in the phenomenological applications of LFD to the quark

model, it is customary to work in the Bakamjian-Thomas construction [22], that is adding a phenomenological interaction to the free mass operator, only. However, the resulting total angular momentum operator, although interaction free, does not satisfy ordinary composition rules. In order to restore them, a unitary transformation of the Hilbert space, known as Melosh Rotation (MR), has to be performed. In particular, if the nucleon is in a S-wave state, such rotation acts only on the spin part of the wave function.

The $D^{1/2}$ representation of the MR is given by:

$$D^{1/2}[R_M(\vec{k})] = \frac{(m + \omega + k_z) - i\vec{\sigma} \cdot (\hat{z} \times \vec{k}_\perp)}{((m + \omega + k_z)^2 + \vec{k}_\perp^2)^{1/2}} . \quad (6)$$

As a result, motion and spin are now intimately correlated as it is required by a relativistic theory. The MR can be interpreted as the boost transformations required to move from the rest frame of each subsystem (quark) to the rest frame of the total system (nucleon).

In the present study we will not investigate $SU(6)$ breaking effects in spin-isospin space: the nucleon wave function will correspond to a S-wave. This simplifying assumption ensures that the non-vanishing OAM contribution originates from pure relativistic effects due to the treatment of the spin in light-front dynamics. Indeed the MR gives rise to a non-vanishing angular momentum density even if the spatial wave function corresponds to a S-wave and the angular momentum density can be written, for a $SU(6)$ symmetric spin-isospin wave function, as

$$L_z(\vec{k}) = \frac{1}{3} \frac{\vec{k}_\perp^2}{(m + \omega + k_z)^2 + \vec{k}_\perp^2} n(\vec{k}) , \quad (7)$$

where $n(\vec{k})$ is the total momentum density, defined in the usual way :

$$n(\vec{k}) = \langle \Psi_N | \sum_{i=1}^3 \delta(\vec{k}_i - \vec{k}) | \Psi_N \rangle , \quad (8)$$

and normalized to the number of particles ($\int n(\vec{k}) d\vec{k} = 3$). Recalling the expressions for the polarized densities that enter the helicity distributions [16, 17]:

$$\begin{aligned} n_u^\uparrow(\vec{k}) - n_u^\downarrow(\vec{k}) &= -4 \left(n_d^\uparrow(\vec{k}) - n_d^\downarrow(\vec{k}) \right) \\ &= \frac{4(m + \omega + k_z)^2 - \vec{k}_\perp^2}{9(m + \omega + k_z)^2 + \vec{k}_\perp^2} n(\vec{k}) , \end{aligned} \quad (9)$$

one can check that the total angular momentum sum rule is automatically fulfilled at the hadronic scale:

$$\frac{1}{2} \int (g_1^u(x, \mu_0^2) + g_1^d(x, \mu_0^2)) dx + \int dx L_z(x, \mu_0^2) = \frac{1}{2}. \quad (10)$$

Another interesting relationship connects L_z to the longitudinal (g_1) and transversity (h_1) parton distributions, namely [14]:

$$g_1^a(x, \mu_0^2) + L_z^a(x, \mu_0^2) = h_1^a(x, \mu_0^2), \quad (11)$$

and is naturally fulfilled in our approach. This relationship also holds for other relativistic models of the nucleon, such as the bag model. Let us stress that Eq. (11) is valid at the hadronic scale μ_0^2 only and one should be careful when using it to extract information about L_z^a because it is broken by evolution, even at small values of Q^2 . This can be easily demonstrated by considering the singlet combination corresponding to Eq. (11), i.e.

$$\Sigma(x, \mu_0^2) + L_z(x, \mu_0^2) - H(x, \mu_0^2) = 0 \quad (12)$$

where $\Sigma(x, \mu_0^2) = \Sigma_a(g_1^a(x, \mu_0^2) + g_1^{\bar{a}}(x, \mu_0^2))$ and $H(x, \mu_0^2) = \Sigma_a(h_1^a(x, \mu_0^2) - h_1^{\bar{a}}(x, \mu_0^2))$ ¹. In order to check the validity of Eq. (11) at $Q^2 > \mu_0^2$ let us evolve (at LO) the first moments of the left-hand side of Eq. (12):

$$\begin{aligned} \langle \Sigma(x, Q^2) \rangle_1 + \langle L_z(x, Q^2) \rangle_1 - \langle H(x, Q^2) \rangle_1 &= \frac{1}{2}(1 - b^{-50/81}) \langle \Sigma(x, \mu_0^2) \rangle_1 \\ &+ (b^{-50/81} - b^{-4/27}) \langle H(x, \mu_0^2) \rangle_1 \\ &+ \frac{9}{50}(1 - b^{-50/81}) \end{aligned} \quad (13)$$

where $b = \frac{\ln(Q^2/\Lambda^2)}{\ln(\mu_0^2/\Lambda^2)}$. Clearly, the right-hand side of the equation above vanishes only if $Q^2 = \mu_0^2$. Furthermore, due to the form of the b -dependent coefficients, it quickly deviates from 0 at the initial stages of evolution pointing out the limits of the attempt, carried out in [14], of extracting information on L_z from Eq. (11).

Coming back to our evaluation of OAM, Eqs. (7) - (9) show that the exact ratio between the amount of OAM and spin will depend on the specific form of $n(\vec{k})$, or equivalently, on the spatial nucleon wave function. Let us note however that the momentum density averages many details of the spatial wave function and to this respect, the sensitivity of the final results to the fine details of the spatial wave function is reduced.

¹The minus sign in front of $h_1^{\bar{a}}$ comes from the properties of the operator that defines the transversity under charge conjugation, and therefore the analogous of Eq. (11) for antiquarks should read $g_1^{\bar{a}}(x, \mu_0^2) + L_z^{\bar{a}}(x, \mu_0^2) = -h_1^{\bar{a}}(x, \mu_0^2)$. Though our model does not contain antiquarks at the scale μ_0^2 , this relationship can be easily checked in the bag model.

In the following we will discuss predictions obtained solving explicitly the mass equation:

$$\hat{M} \Psi = \left(\sum_{i_1}^3 \sqrt{\vec{k}_i^2 + m^2} + V \right) \Psi = E \Psi \quad (14)$$

with an hypercentral phenomenological potential:

$$V = -\frac{\tau}{\xi} + \kappa_l \xi + \Delta \quad , \quad (15)$$

where ξ is the hyperradius defined in the usual way and τ , κ_l and Δ are free parameters that are fixed by spectroscopy requirements [16, 23, 24]. It is worthwhile mentioning that MR has no effects on the energy levels of the confining mass operator (14) - (15) explaining to some extent the success of non-relativistic (or relativized) approaches in reproducing the baryonic spectrum. On the other hand, another remarkable effect of the relativistic mass equation is the enhancement of the high momentum components in the nucleon wave function. Since the MR factor involves momentum dependent terms, the final results will be biased by the presence of these high-momentum components. In order to test the sensitivity to the details of the momentum density we will consider an additional scenario where the MR factors are combined with a wave function obtained from the non-relativistic Schrödinger reduction of the Eq. (14) with the same form of potential (15). This new spatial wave function, hereafter indicated by Ψ' , will contain far less high momentum components. In fact one of the risks of guessing the wave function instead of solving the mass equation (14) explicitly, is to underestimate the contribution coming from the high-momentum components of the correct solution, mostly carried over by the relativistic kinetic energy operator in the mass equation. Although the use of MR is not fully consistent when Ψ' is considered, since it was derived from a non-relativistic mass equation, we will discuss it as a 'pedagogical' example that represents an extreme scenario where high-momentum components have been strongly suppressed. The comparison of results obtained with Ψ and Ψ' will serve to establish bounds on the effects of MR.

3 Results and discussion

The obtained OAM distribution at the hadronic scale μ_0^2 , Eq. (4), for the wave function Ψ , the solution of Eq. (14), is shown in Fig. 1.a. The outcome for the modified scenario (corresponding to the wave function Ψ') is shown in Fig. 1.b to appreciate the effect of the lack of high momentum components. Furthermore, the comparison with the bag model results [13] is also provided (Fig. 1.c). It is clear that the LFCQM, regardless of the details of the spatial

wave function, provides OAM distributions which are comparable (even bigger by a factor 2) to the bag model. From the comparison between Figs. 1.a and 1.b one can see that the MR (and not the specific shape of the spatial wave function) is responsible for this sizeable OAM. In non-covariant quark models such as the Isgur-Karl model, where MR is omitted, the OAM distributions is almost flat [13]. Even when considering a D-model [25] where the probability of the D-wave component is raised up to a 20 %, the resulting OAM, though comparable in size to those obtained here, are peaked at lower x . Nonetheless the large deformation of the nucleon in the D-model should not be taken as realistic.

In order to bring the OAM distributions to the high-energy experimental scale, we use the recently obtained evolution equations at LO [9, 26]. In the process the OAM distributions for the gluons will be generated. The initial scale μ_0^2 is determined following the criteria exposed in [16], and at LO turns out to be $\mu_0^2 = 0.079 \text{ GeV}^2$. In fig. 1.a and 1.b we also present the evolved OAM distributions up to $Q^2 = 10 \text{ GeV}^2$ (short-dashed line) and $Q^2 = 1000 \text{ GeV}^2$ (long-dashed line).

By comparing again the LFCQM with the bag model (Fig. 1.c) it is clear that a non-vanishing OAM persists in the large x region and this is a distinctive feature of relativistic treatments of the nucleon. Indeed, in I-K models, the OAM is entirely concentrated at low x . This may constitute a clear signature of relativity in the low-energy models of the nucleon if $L_z(x, Q^2)$ is measured.

In our approach all the gluon OAM is generated through evolution. In Fig. 2 we present the resulting $L_g(x, Q^2 = 10 \text{ GeV}^2)$ for Ψ , Ψ' and the bag model. There is an inverse correlation between the amount of high momentum components in the wave function and the value of L_g at small x . The OAM gluon distribution for the bag model falls between those obtained with Ψ and Ψ' .

Concerning the first moments of the distributions, our model gives a value for $L_q(\mu_0^2) = \int L_z(x, \mu_0^2) dx$ that ranges from 0.272 to 0.126 (Ψ and Ψ' model respectively). It should be stressed that the corresponding values for $\Delta\Sigma$ (0.456 and 0.748 respectively) are *per se* a clearcut signature in favor of light-front quark models, when compared to recent analysis of data ($\Delta\Sigma = 0.45 \pm 0.09$) [4]. Furthermore, these numbers are quite close to the angular momentum share-out given by the bag model.

The first moments that make up the spin sum rule also evolve with Q^2 according to [26]:

$$\frac{1}{2}\Delta\Sigma(Q^2) = \frac{1}{2}\Delta\Sigma(\mu_0^2) \quad (16)$$

$$L_q(Q^2) = (b^{-\frac{50}{81}} - 1)\frac{1}{2}\Delta\Sigma(\mu_0^2) + b^{-\frac{50}{81}}L_q(\mu_0^2) - \frac{9}{50}(b^{-\frac{50}{81}} - 1) \quad (17)$$

$$J_g(Q^2) = b^{-\frac{50}{81}} J_g(\mu_0^2) - \frac{8}{25} (b^{-\frac{50}{81}} - 1) \quad (18)$$

In Fig. 3 we show the evolution of these quantities with Q^2 for Ψ (Fig. 3.a) and Ψ' (Fig. 3.b). It is worthwhile mentioning that, even if we do not have gluons at the hadronic scale, they quite rapidly develop a sizeable angular momentum content. Furthermore the gluon angular momentum evolves decoupled from the quark sector and if we start with a vanishing $J_g(\mu_0^2)$ then $J_g(Q^2)$ is completely determined by the QCD anomalous dimensions. The values for $J_g(Q^2)$ in the region between 1 and 10 GeV² that we find ($J_g \sim 0.20 - 0.25$) are compatible with those found by using QCD sum rules [27] ($J_g \sim 0.25$) and in a recent lattice calculation [28] ($J_g = 0.20 \pm 0.07$). They also agree with another model calculation based on the one-gluon exchange interaction between quarks [29] ($J_g \sim 0.24$). The consideration of a non-vanishing $J_g(\mu_0^2)$ would not change much our results since it would also raise the scale μ_0^2 (due to the fact that at that scale the gluons would carry some momentum) and hence b would be larger for a given Q^2 .

Though the large error bars in the first direct measurement of the ratio $\frac{\Delta g}{g}$ [30], $\frac{\Delta g}{g} = 0.41 \pm 0.18(stat) \pm 0.03(syst)$, and the values for Δg obtained in recent data analysis [4], $\Delta g(Q^2 = 1 \text{ GeV}^2) = 1.6 \pm 0.9$, do not allow to discriminate between models, our results fall within the range of the latter. As a matter of fact the rather moderate values for J_g result from a strong cancellation between $L_q(Q^2)$ and $\Delta g(Q^2)$ and, in particular we have $\Delta g(Q^2 = 1 \text{ GeV}^2) = 1.36$ and 2.22 for Ψ and Ψ' respectively.

In a non-relativistic quark model one would expect $L_q(Q^2) \sim -J_g(Q^2) \sim -0.25$ in the range $Q^2 \sim 1 - 10 \text{ GeV}^2$ since $\Delta\Sigma$ is a constant with Q^2 . When relativistic spin effects are taken into account, as Fig. 3 shows, one expects $L_q(Q^2)$ to be much smaller ($L_q(Q^2) \sim -0.12$ at most) or close to zero.

4 Concluding remarks

In summary we have shown that covariant light-front based quark models give rise to non-trivial predictions for the OAM distributions at both low and high momentum scales. This departure from traditional treatments of the angular momentum structure of the nucleon is more manifest in the high- x region of the quark sector. We have seen that the performance of LFCQM is quite similar to other relativistic models of the nucleon such as the bag model. This comparison holds for a quite flexible choice of the mass operator. We have studied the predictions for other potentials that interpolate between the two somehow extreme situations presented here and conclusions are not changed. In fact, there is a clear correlation between the amount of high-momentum components in the momentum density $n(\vec{k})$ and the size of the

OAM distribution. A more realistic interaction would give results closer to those of Ψ than to those obtained with Ψ' because a relativistic treatment of the kinetic energy operator inevitably emphasizes the high-momentum tail.

One should keep in mind however that the origin of the relativistic aspects is not the same in the bag and in the LFCQM presented here. While in the former the non-vanishing OAM comes from the small Dirac components, in the latter these ones are absent and relativity enters through the momentum dependence of the Pauli spinors. Certainly other more sophisticated spin-flavour basis can be constructed, such as the Dirac-Melosh bases [31], where covariance is manifest. Despite the fact that the used basis contains only kinematic and not dynamical (higher Fock states) effects, it represents a minimal framework that combines in an elegant way simplicity and a proper treatment of boost. Results obtained with this basis and with the bag model are of similar quality pointing out that it allows an easy implementation of relativistic effects in the spin structure of the nucleon.

We gratefully acknowledge Vicente Vento for useful comments and a careful reading of the manuscript.

References

- [1] EM Collaboration, J. Ashman et al., Phys. Lett. B206 (1988) 364; Nucl. Phys. B328 (1989) 1.
- [2] SM Collaboration, D. Adams et al., Phys. Lett. B329 (1994) 399; erratum ibid. B339 (1994) 332; Phys. Rev. D56 (1997) 5330.
- [3] G. Altarelli, G.G. Ross, Phys. Lett. B212 (1988) 391. R.D. Carlitz, J.C. Collins and A.H. Mueller, Phys. Lett. B214 (1988) 229.
- [4] G. Altarelli, R.D. Ball, S. Forte and G. Ridolfi, Nucl. Phys. B496 (1997) 337.
- [5] L.M. Sehgal, Phys. Rev. D10 (1974) 1663;
- [6] R.L. Jaffe and A. Manohar, Nucl. Phys. B337 (1990) 509.
- [7] For a recent review: B. Lampe and E. Reya, 'Spin Physics and Polarized Structure Functions', hep-ph/9810270.
- [8] P.G. Ratcliffe, Phys. Lett. B192 (1987) 180.
- [9] X. Ji, Phys. Rev. Lett. 78 (1997) 610; P. Hoodbhoy, X. Ji and W. Lu, Phys. Rev. D59, (1999), 014013.

- [10] S.V. Bashinsky and R.L. Jaffe, Nucl. Phys. B 536, (1998), 303.
- [11] X. Ji, J. Tang and P. Hoodbhoy, Phys. Rev. Lett. 76 (1996) 740; P. Hägler and A. Schäfer, Phys. Lett. B430 (1998) 179; A. Harindranath and R. Kundu, Phys. Rev. D59, 116013, (1999). O.E. Teryaev, hep-ph/9803403.
- [12] P. Hoodbhoy, X. Ji and W. Lu, Phys. Rev. D 59, 074010, (1999).
- [13] S. Scopetta and V. Vento, Phys. Lett. B 460 (1999) 8; Erratum (to appear).
- [14] B.-Q. Ma and I. Schmidt, Phys. Rev. D58, 096008 (1999).
- [15] B.-Q. Ma and Q.-R. Zang, Z. Phys. C58 (1993) 479; S.J. Brodsky and F. Schlumpf, Phys. Lett. B329 (1994) 111; B.-Q. Ma, I. Schmidt and J. Soffer, Phys. Lett. B 441, (1998), 461. M.Wakamatsu and T. Watabe, hep-ph/9912500.
- [16] M. Traini, P. Faccioli and V. Vento, Few-Body Sys. Suppl. 11 (1999) 347; P. Faccioli, M. Traini and V. Vento, Nucl. Phys. A656 (1999) 400.
- [17] F. Cano, P. Faccioli and M. Traini, hep-ph/9902345.
- [18] M. Traini, L. Conci and U. Moschella, Nucl. Phys. A544 (1992) 731; M. Traini, V. Vento, A. Mair and A. Zambarda, Nucl. Phys. A614 (1997) 472 and references therein.
- [19] A. Mair and M. Traini, Nucl. Phys. A624 (1997) 564; Nucl. Phys. A628 (1998) 296.
- [20] S. Scopetta, V. Vento and M. Traini, Phys. Lett. B421 (1998) 64; Phys. Lett. B442 (1998) 28.
- [21] N. Isgur and G. Karl, Phys. Rev. D18 (1978) 4187; D19 (1979) 2653; D23 (1981) 817 (Erratum).
- [22] B.D. Keister and W.N. Polyzou, Adv. in Nucl. Phys. 20 (1991) 225; F. Coester, Prog. Part. Nucl. Phys. 29 (1992) 1; J. Carbonell, B. Desplanques, V.A. Karmanov and J.-F. Mathiot, Phys. Rep. 300 (1998) 215. S.J. Brodsky, H.-C. Pauli and S.S. Pinsky, Phys. Rep. 301 (1998) 299.
- [23] Paolo Longinotti, Tesi di Laurea 1999, unpublished; M. Traini and P. Longinotti, in preparation.
- [24] M. Ferraris, M.M. Giannini, M. Pizzo, E. Santopinto and L. Tiator, Phys. Lett. B364 (1995) 231.

- [25] M. Ropele, M. Traini and V. Vento, Nucl. Phys. A584 (1995) 634.
- [26] O. Martin, P. Hägler and A. Schäfer, Phys. Lett. B 448 (1999) 99.
- [27] I.I. Balitsky and X. Ji, Phys. Rev. Lett. 79 (1997) 1225.
- [28] N. Mathur, S.J. Dong, K.F. Liu, L. Mankiewicz and N. Mukhopadhyay, hep-ph/9912289.
- [29] V. Barone, T. Calarco and A. Drago, Phys. Lett. B431 (1998) 405.
- [30] HERMES Collaboration, A. Airapetian *et al*, hep-ex/9907020 (1999).
- [31] M. Beyer, C. Kuhrts and H.J. Weber, Annals Phys. 269 (1998) 129.

Figure captions

Figure 1 Quark orbital angular momentum distributions calculated in light-front dynamics with the wave function Ψ (a), with the modified wave function Ψ' (see text) (b) and in the bag model (c). Solid lines correspond to the initial hadronic scale μ_0^2 , short-dashed lines to $Q^2 = 10 \text{ GeV}^2$ and long-dashed ones to $Q^2 = 1000 \text{ GeV}^2$.

Figure 2. Gluon orbital angular momentum distributions calculated at $Q^2 = 10 \text{ GeV}^2$ with the wave function Ψ (solid line), Ψ' (long-dashed line) and the bag model (short-dashed line).

Figure 3. The contributions to the proton spin sum rule according to the model with Ψ (a) and Ψ' (b). The dashed curve shows $\frac{1}{2}\Delta\Sigma(Q^2)$, the long-dashed one is $L_q(Q^2)$ and the dot-dashed curve represents $J_g(Q^2)$.

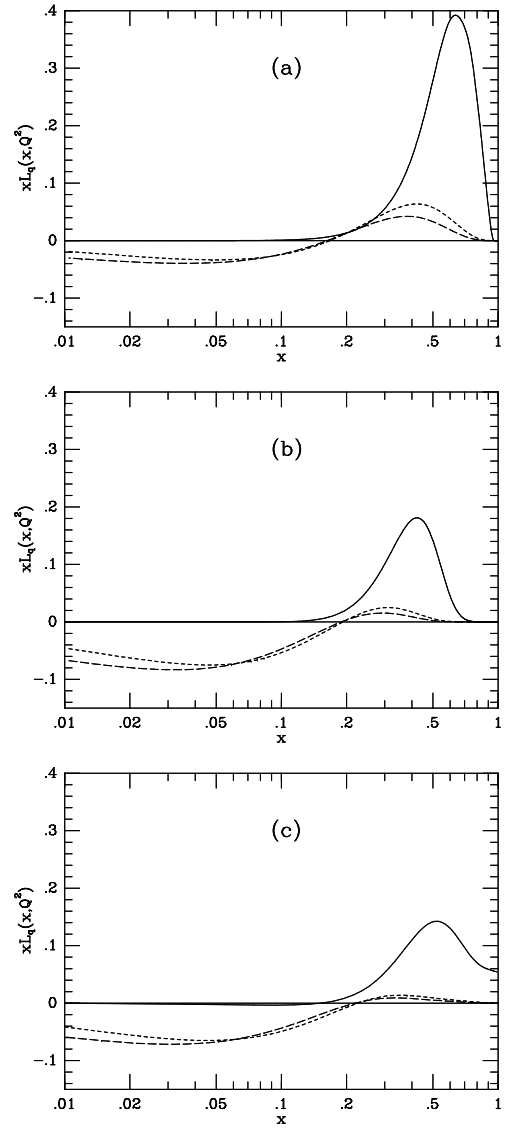


Figure 1

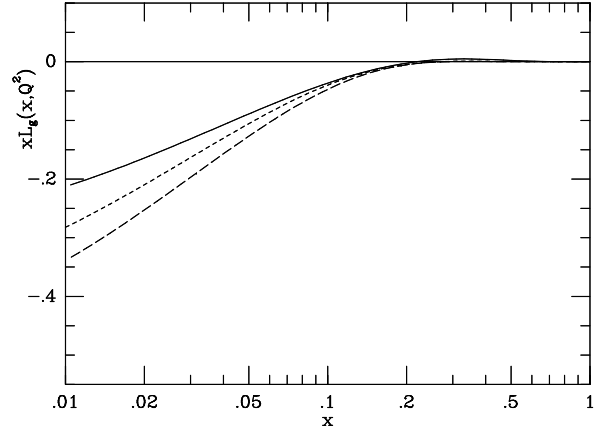


Figure 2

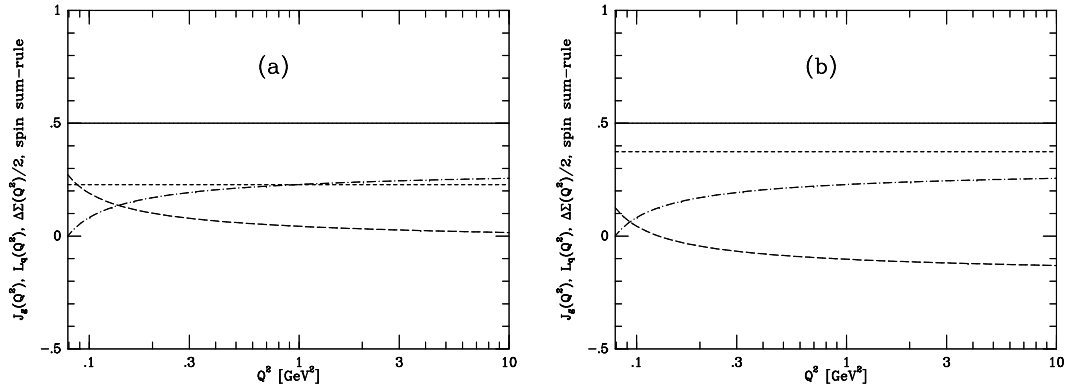


Figure 3